In Situ Observation of the Effect of Nitrogen on Carbon Nanotube Synthesis

ARTICLE *in* CHEMISTRY OF MATERIALS · FEBRUARY 2013

Impact Factor: 8.35 · DOI: 10.1021/cm401216q

7 AUTHORS, INCLUDING:

Rosa E Diaz
Okinawa Institute of Science and Technology
26 PUBLICATIONS **462** CITATIONS
SEE PROFILE

Caterina Ducati
University of Cambridge
176 PUBLICATIONS **6,392** CITATIONS
SEE PROFILE

Eric Andrew Stach
Brookhaven National Laboratory
392 PUBLICATIONS **15,805** CITATIONS
SEE PROFILE

Krzysztof Koziol
University of Cambridge
125 PUBLICATIONS **1,963** CITATIONS
SEE PROFILE

CHEMISTRY OF MATERIALS

Communication

pubs.acs.org/cm

In Situ Observation of the Effect of Nitrogen on Carbon Nanotube Synthesis

Sebastian W. Pattinson,*[,†] Rosa E. Diaz,[‡] Nadia A. Stelmashenko,[†] Alan H. Windle,[†] Caterina Ducati,[†] Eric A. Stach,[‡] and Krzysztof K. K. Koziol*[,†]

[†]Department of Materials Science and Metallurgy, University of Cambridge, Cambridge, CB2 3QZ, United Kingdom

[‡]Center for Functional Nanomaterials, Brookhaven National Laboratory, Upton, New York 11973-5000, United States

Supporting Information

KEYWORDS: *carbon nanotube synthesis, nitrogen carbon nanotubes, environmental TEM, chemical vapor deposition*

Control over carbon nanotube (CNT) properties including chiral angle, length, areal density, and diameter is crucial for applications ranging from fibers[1] to separation membranes.[2] A primary avenue of research into enhancing CNT properties has been the use of heteroatoms. Often this has been nitrogen,[3−7] but others such as sulfur,[1] phosphorus,[8] and boron[9] have also been used. Nitrogen is prominent because it can affect diverse CNT properties when added to synthesis, including field-emission,[3] dispersibility,[4] and catalytic activity.[5] Nitrogen can also affect the synthesis process more directly and has been shown, for instance, to alter the chiral angle of CNTs,[6,7] reduce CNT growth rate,[10] increase nanotube areal density,[7] and increase or decrease the crystallinity of nanotube walls.[6,7] We have also previously shown that many nitrogen forms allow the production of multiwalled CNTs in which every layer has an identical chiral angle and have proposed a synthesis mechanism for these CNTs relying on their growth from an oriented Fe_3C catalyst particle containing a restructured pure iron surface that is epitaxially matched to the CNT.[6,7] That nitrogen addition to CNT synthesis causes such diverse and useful effects suggests a need to understand how it affects this process.

Environmental TEM (ETEM) is a relatively new technique ideal for in situ measurements.[11] We apply ETEM to study the effect of nitrogen on CNT growth, elucidating the mechanisms by which nitrogen acts, to guide efforts to optimize synthesis. To the best of our knowledge, this is the first in situ TEM study of the effect of nitrogen on CNT growth.

Iron layers between 0.1 and 2.5 nm thick were sputter deposited onto amorphous 20 nm thick silicon dioxide membranes (SIMPore). Typically, the membranes would be introduced into the environmental microscope (FEI Titan 80/300 E-TEM, equipped with a CEOS postspecimen aberration corrector), heated to 650 °C, and then treated in 100−200 mTorr hydrogen for 10 min. Next, acetylene and ammonia were added to begin CNT growth. Ammonia is compatible with the microscope and likely to be completely dissociated on the catalyst,[7] meaning that these results should also apply to other nitrogen sources, insofar as they can supply similar nitrogen activity. Typical reaction gas pressure in the microscope was between 2 and 30 mTorr. Bulk CNT array growth rate measurements were taken of CNTs grown with feedstock of 5 wt % ferrocene in 95 wt % toluene, and 5 wt % ferrocene, 75 wt % toluene, and 20 wt % pyrazine in a CVD furnace at 760 °C, with argon as carrier gas flowing at 0.8 L/min. A laser extensometer was used for growth rate measurements using a previously described setup.[12]

The addition of a small relative pressure of ammonia (between 1:100 and 1:10 NH_3:C_2H_2 pressure ratio) to the microscope during CNT growth had no noticeable effect on the synthesis process. Increasing the relative ammonia pressure to 1:1 NH_3 C_2H_2, however, had a marked effect on CNT nucleation and growth. CNT nucleation initially involves the nucleation of a graphene cap from the catalyst, which forms the tip of the nanotube. With very low ammonia concentration the cap separates from the catalyst immediately following precipitation (Figure 1a). At higher ammonia concentration the carbon layer remains in contact with the catalyst it precipitated from throughout nucleation and growth (Figure 1b).

That the catalyst remains in contact with the CNT even after nucleation at higher nitrogen concentration suggests that nitrogen decreases the interface energy between the catalyst and the CNT. In general, high chemical potential nitrogen sources, such as ammonia, reduce the driving force for graphite precipitation, stabilizing Fe_3C.[7,13] Therefore, with a higher ammonia concentration, the CNT will nucleate on carbide catalyst. By contrast, the activity required for carbon precipitation from iron is lower than it is for the formation of graphite.[14] Therefore, in the absence of ammonia, carbon should precipitate first, resulting in an interface with pure iron. Pure iron has a higher surface tension with the nanotube, which explains the separation of the CNT and catalyst immediately following carbon precipitation.[11] A carbide particle will have a lower surface tension with the nanotube due to its higher carbon chemical potential and thus maintain its contact.[15] The pure iron catalyst may become carbide following cap separation, but this will not affect CNT nucleation.

Ammonia concentration also strongly affects catalyst morphology during growth. With less ammonia, the catalyst

Received: April 15, 2013
Revised: July 17, 2013
Published: July 25, 2013

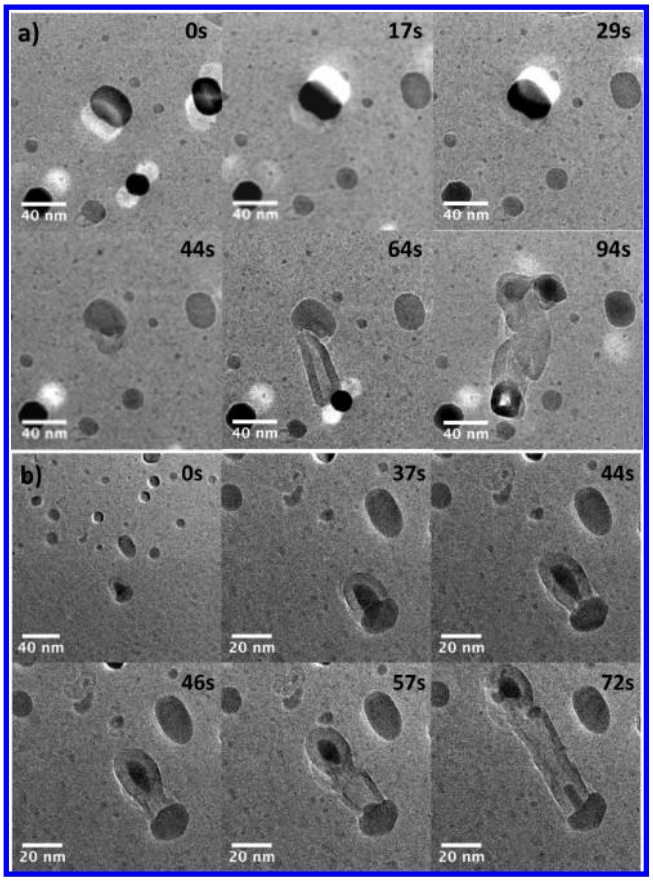

Figure 1. (a) TEM image sequence, with time intervals displayed, showing the nucleation of a CNT from a catalyst particle in a 20:1 C_2H_2:NH_3 atmosphere. Also visible in the final frame is the deformation of the catalyst particle that occurs during growth. (b) Sequence of TEM images showing the nucleation of a CNT from catalyst in 1:1 C_2H_2:NH_3.

deforms significantly and is highly mobile with an average lateral movement of 3.5 nm/s and even appears to lift off the substrate (Figure 2). Increasing the ammonia concentration causes the active catalyst to remain firmly rooted to the substrate with no measurable lateral movement and also to maintain a more constant shape. While the increase in ammonia concentration keeps the catalyst stationary, the fast Fourier transforms (FFTs) of the lattice fringes in the marked catalyst particle in Figure 2b suggest that the orientation of the catalyst is, nevertheless, constantly changing, and that it is carbide. At 86 s, the lattice fringes are most closely compatible with the [513] orientation of Fe_3C. At 91 s, spacing in the particle of 0.37 nm is visible, which is compatible with the $(0\bar{1}1)$ reflection of Fe_3C, and incompatible with either FCC or BCC iron. At 144 s spacing of 0.25 nm is visible in the marked particle, again only compatible with Fe_3C.

Video recordings also allow an estimate of how ammonia concentration affects the number of carbon atoms emerging from the catalyst by measuring the thickness of the CNT walls, the length of the CNT grown per second, and the cross-sectional area of the catalyst (Figure 3). The average carbon flux from catalyst at low ammonia is approximately 4 times higher than that from catalyst grown at high ammonia concentration. The standard deviation in carbon flow as a percentage of the average flow rate at low ammonia is 58% and 51% at high ammonia, suggesting that the carbon extrusion rate

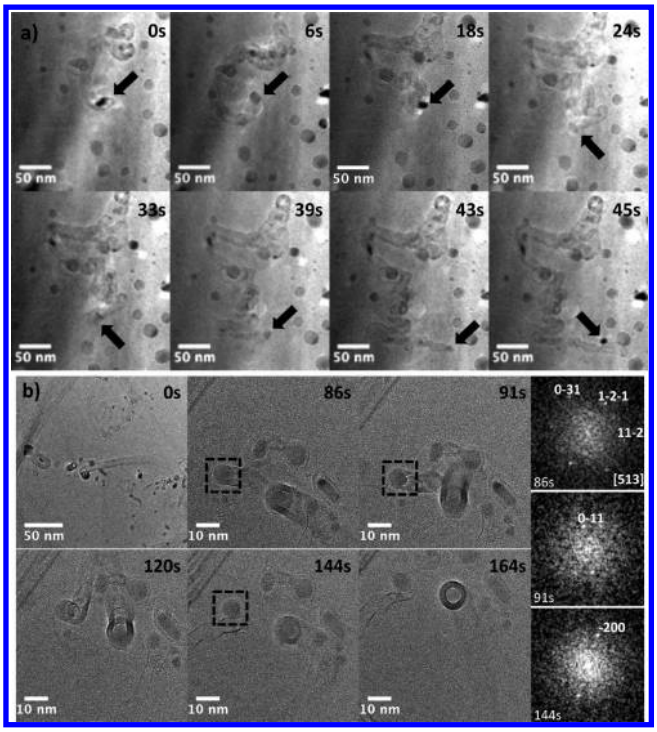

Figure 2. (a) Sequence of TEM images of CNT growth in a 20:1 C_2H_2:NH_3 atmosphere and (b) sequence taken in 1:1 C_2H_2:NH_3. Marked catalyst particles display lattice fringes with FFTs shown.

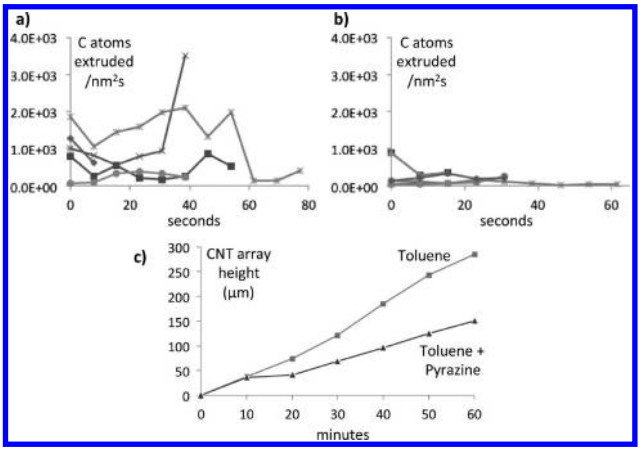

Figure 3. Graphs showing the number of carbon atoms extruded per nm^2 of catalyst cross-sectional area per second for (a) five CNTs grown under low nitrogen conditions and (b) high nitrogen conditions. (c) Growth rates of CNT arrays grown with and without a nitrogen source (pyrazine), measured by laser extensometer.

is similarly uneven irrespective of nitrogen concentration. The average growth rate in CNT length at low ammonia concentration was 5.9 nm/s, while at high ammonia concentration it was 3.4 nm/s. These measurements may be affected by factors, such as the electron beam, that are peculiar to the ETEM environment.[16] However, a decrease in growth rate is also seen in CNT arrays in a bulk CVD reactor upon the addition of nitrogen sources (Figure 3c).

The kinetic results therefore strongly suggest that the addition of nitrogen sources slows CNT growth rate, as already reported,[10] by reducing the carbon extrusion rate from catalyst. The decrease in carbon extrusion rate of approximately 75% resulting from the addition of nitrogen is too small to be caused

dx.doi.org/10.1021/cm401216q | *Chem. Mater.* 2013, 25, 2921−2923

by a difference in the iron phase from which the catalyst grows.[17,18] It has also been suggested that a decrease in the growth rate of CNTs grown in the presence of a nitrogen source could be due to saturation of the growing CNT edge with nitrogen.[19] This slows CNT growth because the nitrogen must be either substituted by carbon or form defects in the nanotube. Given that our catalyst is Fe_3C during growth, though, and that the solubility of nitrogen in Fe_3C is negligible,[20] it seems unlikely that sufficient nitrogen would diffuse through the catalyst to cause such a blockage in our system. We suggest that the low solubility of nitrogen in Fe_3C in a high ammonia concentration atmosphere results in a buildup of nitrogen at the catalyst surface exposed to the reactants. This reduces the carbon deposition efficiency on the catalyst and thus CNT growth rate. The thinner walls of CNT samples grown in high ammonia (average 3.1 nm thickness compared to 8.2 nm in low nitrogen) also suggest that higher nitrogen causes less carbon to be available to the growing CNT. The lower carbon extrusion rate likely decreases the mechanical forces on the catalyst, leading to morphological stability.

Our ETEM study suggests that increased nitrogen concentration affects both the nucleation and the growth of CNTs. Nitrogen reduces surface energy at the catalyst/CNT interface, reduces carbon extrusion from the catalyst and thus CNT growth rate, reduces catalyst motion, and stabilizes catalyst morphology during growth. These mechanisms help to explain how the addition of nitrogen to synthesis is able to improve important CNT characteristics. Nitrogen stabilizes the interface between the catalyst and the nanotube through the decrease in interface energy, as well as a more constant catalyst morphology and reduced lateral movement of the catalyst. This is likely to contribute both to the ability of nitrogen to affect CNT chiral angle through epitaxy with the catalyst[7] and its ability to increase nanotube crystallinity.[6] Similarly, the decrease in lateral movement of the catalyst may allow catalyst particles to grow in high areal density without coalescing, accounting for the high CNT densities observed when nitrogen is used in synthesis.[7] This effect could also be used to increase nanotube diameter uniformity. The mechanisms by which nitrogen acts on the catalyst during growth can also be effected by different means to improve CNT, and other nanowire, properties. For instance, the use of novel, porous substrates[21] could improve catalyst stability, and adding surface-active atoms to synthesis could further reduce the surface tension at the catalyst/nanotube interface.

■ ASSOCIATED CONTENT

Supporting Information

Video recordings of CNT growth are included. This material is available free of charge via the Internet at http://pubs.acs.org.

■ AUTHOR INFORMATION

Corresponding Author

*E-mail: swp29@cam.ac.uk (S.W.P.); kk292@cam.ac.uk (K.K.K.K.).

Notes

The authors declare no competing financial interest.

■ ACKNOWLEDGMENTS

The authors thank Hajime Murakami for taking extensometer measurements. S.W.P. thanks the EPSRC for funding. K.K.K.K. and C.D. thank the Royal Society and ERC for funding. In situ microscopy took place at the Center for Functional Nanomaterials, Brookhaven National Laboratory, which is supported by the U.S. Department of Energy, Office of Basic Energy Sciences, under Contract No. DE-AC02-98CH10886.

■ REFERENCES

(1) Li, Y.-L.; Kinloch, I. A; Windle, A. H. *Science* **2004**, *304*, 276−278.
(2) Hinds, B. J.; Chopra, N.; Rantell, T.; Andrews, R.; Gavalas, V.; Bachas, L. G. *Science* **2004**, *303*, 62−65.
(3) Tang, C.; Golberg, D.; Bando, Y.; Xu, F.; Liu, B. *Chem. Commun.* **2003**, 3050−3051.
(4) Kim, J. H.; Kataoka, M.; Fujisawa, K.; Tojo, T.; Muramatsu, H.; Vega-Díaz, S. M.; Tristán-López, F.; Hayashi, T.; Kim, Y. A.; Endo, M.; Terrones, M.; Dresselhaus, M. S. *J. Phys. Chem. B* **2011**, *115*, 14295−14300.
(5) Gong, K.; Du, F.; Xia, Z.; Durstock, M.; Dai, L. *Science* **2009**, *323*, 760−764.
(6) Koziol, K. K. K.; Ducati, C.; Windle, A. H. *Chem. Mater.* **2010**, *22*, 4904−4911.
(7) Pattinson, S. W.; Ranganathan, V.; Murakami, H. K.; Koziol, K. K. K.; Windle, A. H. *ACS Nano* **2012**, *6*, 7723−30.
(8) Jourdain, V.; Stéphan, O.; Castignolles, M.; Loiseau, A.; Bernier, P. *Adv. Mater.* **2004**, *16*, 447−453.
(9) Redlich, P.; Loeffler, J.; Ajayan, P. M.; Bill, J.; Aldinger, F.; Ruhle, M. *Chem. Phys. Lett.* **1996**, *260*, 465−470.
(10) Koós, A. A.; Dowling, M.; Jurkschat, K.; Crossley, A.; Grobert, N. *Carbon* **2009**, *47*, 30−37.
(11) Wirth, C. T.; Bayer, B. C.; Gamalski, A. D.; Esconjauregui, S.; Weatherup, R. S.; Ducati, C.; Baehtz, C.; Robertson, J.; Hofmann, S. *Chem. Mater.* **2012**, *24*, 4633−4640.
(12) Pattinson, S. W.; Prehn, K.; Kinloch, I. a.; Eder, D.; Koziol, K. K. K.; Schulte, K.; Windle, A. H. *RSC Adv.* **2012**, *2*, 2909−2913.
(13) Gressmann, T.; Nikolussi, M.; Leineweber, A.; Mittemeijer, E. J. *Scr. Mater.* **2006**, *55*, 723−726.
(14) Szakalos, P. *Mater. Corros.* **2003**, *54*, 752−762.
(15) Zhang, X.; Li, Z.; Wen, G.; Fung, K.; Chen, J.; Li, Y. *Chem. Phys. Lett.* **2001**, *333*, 509−514.
(16) Wirth, C.; Zhang, C.; Zhong, G.; Hofmann, S.; Robertson, J. *ACS Nano* **2009**, *3*, 3560−3566.
(17) Thibaux, P.; Métenier, A.; Xhoffer, C. *Metall. Mater. Trans. A* **2007**, *38*, 1169−1176.
(18) Schneider, A.; Inden, G. *Calphad* **2007**, *31*, 141−147.
(19) Sumpter, B. G.; Meunier, V.; Romo-Herrera, J. M.; Cruz-Silva, E.; Cullen, D. A.; Terrones, H.; Smith, D. J.; Terrones, M. *ACS Nano* **2007**, *1*, 369−375.
(20) Nikolussi, M.; Leineweber, A.; Mittemeijer, E. J. *Philos. Mag.* **2010**, *90*, 1105−1122.
(21) Pattinson, S. W.; Windle, A. H.; Koziol, K. K. K. *Mater. Lett.* **2013**, *93*, 404−407.